

Synthesis and Characterization of Poly(ethylene glycol) Diacrylate Copolymers Containing Azobenzene Groups Prepared by Frontal Polymerization

JAVIER ILLESCAS,^{1,2} YESSICA S. RAMIREZ-FUENTES,¹ ERNESTO RIVERA,¹ OMAR G. MORALES-SAAVEDRA,³ ANTONIO A. RODRÍGUEZ-ROSALES,³ VALERIA ALZARI,² DANIELE NUVOLE,² SERGIO SCOGNAMILLO,² ALBERTO MARIANI²

¹Instituto de Investigaciones en Materiales, Universidad Nacional Autónoma de México. Circuito exterior S/N. Ciudad Universitaria C.P. 04510 México D.F.

²Dipartimento di Chimica, Università di Sassari, and local INSTM Unit, Via Vienna 2, 07100 Sassari, Italy

³Centro de Ciencias Aplicadas y Desarrollo Tecnológico, Universidad Nacional Autónoma de México, Circuito exterior S/N. Ciudad Universitaria C.P. 04510 México D.F.

Received 7 April 2011; accepted 7 May 2011

DOI: 10.1002/pola.24765

Published online 23 May 2011 in Wiley Online Library (wileyonlinelibrary.com).

ABSTRACT: A novel polymer matrix containing amino–nitro substituted azobenzene groups was obtained by frontal polymerization. (E)-2-(Ethyl(4-((4-nitrophenyl)diazenyl)phenyl)amino)ethyl methacrylate (MDR-1) was copolymerized with poly(ethylene glycol) diacrylate (PEGDA) using this easy and fast polymerization technique. The effect of the amount of the incorporated azo-monomer into the polymer matrix was studied in detail and correlated to front velocity, maximum temperature, initiator concentration, and monomer conversion. The obtained materials were characterized by infrared spectroscopy (Fourier transform infrared), and their thermal properties were studied by thermogravimetric analysis and differential scanning calorimetry. Moreover, the optical properties of the polymers were studied by absorption

spectroscopy in the UV–Vis region. Absorption spectra of the copolymers exhibit a significant blue shift of the absorption bands with respect to the azo-monomer, due to the presence of H-aggregates. Cubic nonlinear optical (NLO) characterizations of the PEGDA/MDR-1 copolymers were performed according to the Z-Scan technique. It has been proven that samples with higher MDR-1 content (0.75 mol %) exhibited outstandingly high NLO-activity with negative NLO-refractive coefficients in the promising range of $n_2 = -8.057 \times 10^{-4}$ esu. © 2011 Wiley Periodicals, Inc. *J Polym Sci Part A: Polym Chem* 49: 3291–3298, 2011

KEYWORDS: azo polymers; frontal polymerization; nonlinear optical; poly(ethylene glycol) diacrylate; radical polymerization

INTRODUCTION In the last 20 years, frontal polymerization (FP) has attracted the attention of the scientific community. In general, it begins with a localized reaction ignited by an external heating or UV-light source. FP was carried out for the first time in 1972 by Chechilo et al.,¹ who polymerized methyl methacrylate (MMA) using benzoyl peroxide (BPO) as initiator. They studied the effects of pressure and initiator concentration over the propagating front speed. Since this early work, FP has evolved in such a way that many research groups have gotten involved in this field. Davtyan et al.² published a first review about FP covering all the literature up to 1984 and studied the gel effect on the frontal radical polymerization of MMA.³ Later, Pojman et al.⁴ got implicated in this research field and published a review covering the most important trends in FP up to 1996. Among other aspects, they investigated the formation of simultaneous-interpenetrating polymer networks,⁵ the influence of the reactor geometry and the spin modes in FP,⁶ the use of a microencapsulated initiator,^{7,8} the FP of various acrylic monomers,^{9–13} urethane-acryl-

ates,¹⁴ poly(dicyclopentadiene),¹⁵ epoxy resins, and more recently, their frontal cationic curing.^{16,17} Finally, some ionic liquids were also studied.¹⁸ Our research group has used FP to obtain unsaturated polyester/styrene resins,¹⁹ diurethane acrylates,²⁰ and polyurethanes,^{21,22} polymer-based nanocomposites with montmorillonite,²³ and polyhedral oligomeric silsesquioxanes,²⁴ interpenetrating polymer networks,²⁵ the consolidation of porous materials,^{26–29} and different kinds of hydrogels.^{30–33} Recently, we proposed FP as a novel method to obtain stimuli responsive hydrogels containing partially exfoliated graphite³⁴ and for the preparation of hybrid inorganic/organic epoxy resins.³⁵

Chen and coworkers have worked on this field using FP for the polymerization of vinylpyrrolidone,³⁶ 2-hydroxyethyl acrylate,³⁷ *N*-methylolacrylamide,³⁸ epoxy resin/polyurethane networks,³⁹ polyurethane-nanosilica hybrid nanocomposites⁴⁰ and quantum dot polymer nanocomposites.⁴¹ Lately, they have also synthesized hydrogels of *N*-vinylimidazole for adsorption of metals⁴² and amphiphilic gels.⁴³ Crivello and

Correspondence to: E. Rivera (E-mail: riverage@iim.unam.mx) or A. Mariani (E-mail: mariani@uniss.it)

Journal of Polymer Science Part A: Polymer Chemistry, Vol. 49, 3291–3298 (2011) © 2011 Wiley Periodicals, Inc.

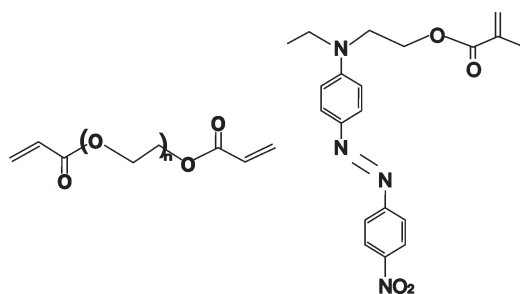


FIGURE 1 Structures of PEGDA (left) and MDR-1 (right).

coworkers reported a new strategy to monitor propagating fronts in the photo-initiated cationic FPs, focusing their research mainly on epoxide monomers.^{44–47}

In a very recent article, we demonstrated that FP can be a technique exploitable to obtain materials that cannot be prepared by the classical method, i.e., graphene-containing nanocomposite hydrogels of poly(*N*-isopropylacrylamide) were synthesized. At variance to what happened during the classical polymerization occurrence, because of the fast monomer into polymer conversion, graphene did not reaggregate to graphite flakes, thus allowing obtaining a homogeneously dispersed nanocomposite.⁴⁸

Poly(ethylene glycol) diacrylate (PEGDA; Fig. 1) is a monomer that has been primarily used in biomaterials science for the elaboration of phase-separation membranes for proteins, as adsorbent of metallic ions in different kinds of solutions or in drug delivery applications. Particularly, this monomer has been of tremendous interest because of its suitability to prepare hydrogels able to respond to external stimuli such as pH or temperature changes.^{49,50}

On the other side, azopolymers have been considered as highly versatile materials due to the photo-induced motions which occur on them, when they are irradiated with laser polarized light.⁵¹ Besides, these polymers exhibit nonlinear optical (NLO)-properties of second and third order; for instance, second harmonic generation (SHG) and third harmonic generation, which make them attractive prospects for the elaboration of optoelectronic devices.⁵² Several reviews covering most of the implications of azobenzene in polymer structures have been published.^{51–56} In the last years, various azo-polymers bearing amino-nitro substituted azobenzene units have been synthesized and characterized.^{57,58} In general, they exhibit absorption maximum wavelengths close to those reported for similar push-pull azo-compounds.^{59,60} In these materials, both J- and H-type aggregations have been observed in cast films.^{58,61} This phenomenon can be exploited for optical applications such as optical storage and photolithography.

In this article, we report the FP of PEGDA, using BPO as initiator. In addition, we have incorporated (E)-2-(ethyl(4-((4-nitrophenyl)diazenyl)phenyl)amino)ethyl methacrylate (named here MDR-1) as a model comonomer. FP was chosen in that it is much easier and faster if compared with the classical routes. The polymers were characterized by Fourier

transform infrared (FTIR) spectroscopy; their thermal properties were determined by thermogravimetric analysis (TGA) and differential scanning calorimetry (DSC), and their optical properties were studied by absorption spectroscopy in the UV-Vis range. Finally, the cubic NLO-characterizations of the PEGDA/MDR-1 copolymers were performed according to the Z-Scan technique.

RESULTS AND DISCUSSION

The results of the FP of PEGDA performed under various reaction conditions are summarized in Table 1. The data refer to BPO concentrations ≥ 0.6 mol %, which is the minimum value that allows the front to self-sustain. It was found that at higher BPO concentrations a faster V_f is observed, ranging from 0.68 cm min^{-1} for 0.6 mol % BPO to 1.90 cm min^{-1} , when the initiator concentration was 7.1 mol %. In the same range, T_{max} slightly increases from 150 to 168 °C.

To obtain a polymer material having possible relevance for future NLO applications, various copolymers of PEGDA and MDR-1 were prepared. It is very well known that azo-polymers bearing a noncentrosymmetric molecular structure, as well as electron-donor and electron-acceptor groups, may exhibit NLO properties such as SHG⁵² when ordered in macroscopic polar structures (for instance in electrically poled or Z-type Langmuir-Blodgett films). In this respect, a concentration of MDR-1 that does not exceed 1.2 mol % was considered adequate. A series of preliminary runs were performed to determine the initiator concentration range that allows the front to self sustain for a MDR-1 content up to 1.2 mol %. Because of the moderate reactivity of azo-monomers such as MDR-1 toward polymerization,⁶² the minimum amount of BPO necessary for the FP to occur was higher than that used for the homopolymerization of PEGDA (i.e., 2.4 instead of 0.6 mol %). Figure 2 shows the data obtained by increasing the MDR-1 content up to 0.75 mol %, keeping the BPO concentration equal to 2.4 mol %. As it can be seen, both V_f and T_{max} decrease as the concentration of MDR-1 augments, thus confirming the aforementioned moderate reactivity of the azo-monomer. Specifically, V_f goes from 1.32 to 0.62 cm min^{-1} as the MDR-1 concentration increases from 0 to 0.75 mol %. As well, T_{max} decreases from 161 to 140 °C in the same range of concentrations.

All samples were characterized by DSC and TGA. In particular, by DSC, it was found that conversions were almost

TABLE 1 V_f , T_{max} , Conversion, and T_g for the FP of PEGDA, Varying the Initiator Concentration

Sample	BPO (mol %)	V_f (cm min ⁻¹)	T_{max} (°C)	Conversion (%)	T_g (°C)
1	0.6	0.68	150	98	-21
2	1.2	1.00	158	94	-24
3	2.4	1.32	161	85	-20
4	4.7	1.40	158	95	-25
5	7.1	1.90	168	84	-26

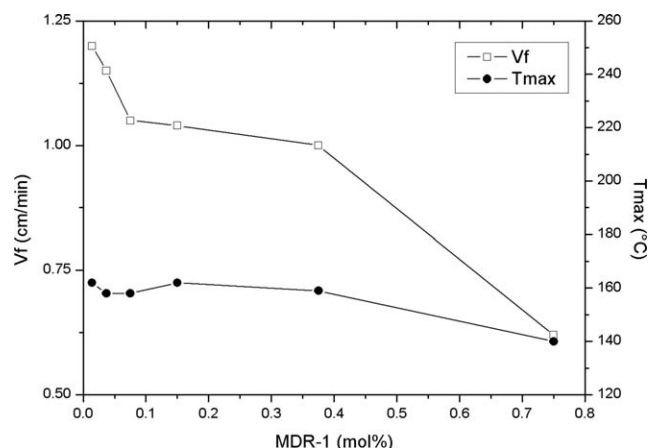


FIGURE 2 V_f and T_{max} for the frontal copolymerization of MDR-1 with PEGDA [BPO: 2.4 mol %] as functions of the MDR-1 concentration.

quantitative, and T_g values were always between -26 and -20 °C, thereby suggesting that neither BPO nor MDR-1 concentrations affect these parameters in a remarkable way (Table 1).

Figure 3 shows the TGA of the PEGDA matrix and of two copolymers with different MDR-1 content. Actually, since the polymerizations occur only with low MDR-1 concentrations, the TGA curves of the obtained copolymers are very similar to that of PEGDA. Indeed, the incorporation of MDR-1 does not affect significantly the thermal stability of the PEGDA matrix, even though the amount of the azo-monomer was increased up to 0.75 mol %. In fact, PEGDA matrix shows a T_{10} value of 363 °C, slightly lower than that observed for the copolymer ($T_{10} = 385$ °C), which can be attributed to a plasticizing effect of MDR-1. All polymers exhibited good thermal stability showing drastic degradation between 400 and 500 °C.

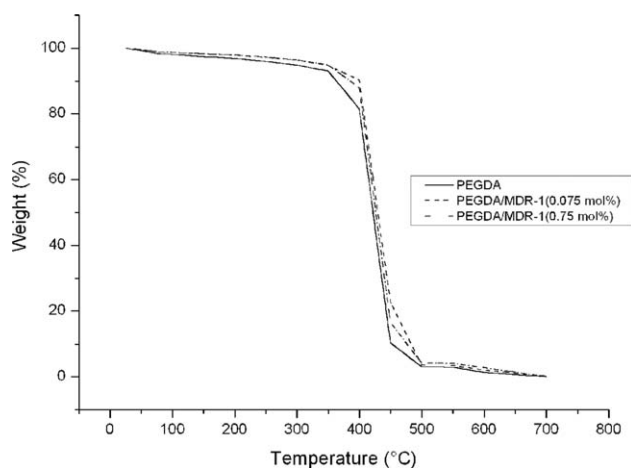


FIGURE 3 TGA of PEGDA polymer matrix and the copolymers with different MDR-1 concentrations [0.075 and 0.75 mol %] [BPO: 2.4 mol %].

The FTIR-spectra of MDR-1 monomer and the polymers are shown in Figure 4. The characteristic bands of the MDR-1 are indicated in the experimental section. The FTIR spectrum of the PEGDA matrix exhibits characteristic bands at $\nu = 2896$ (s, CH_2), 1743 (s, $\text{C}=\text{O}$), 1267 (s, $\text{C}-\text{O}$ ester), and 1116 (s, $\text{O}-\text{CH}_2$) cm^{-1} .

Moreover, the FTIR spectra of MDR-1/PEGDA copolymers with different azobenzene contents were recorded. If we analyze the spectrum of the MDR-1/PEGDA 0.75 mol % copolymer, we can observe a series of bands at 2910 (s, CH_2 , CH_3), 1741 (s, $\text{C}=\text{O}$), 1652 (s, $\text{C}=\text{C}$ aromatic), 1268 (s, $\text{C}-\text{O}$ ester), and 1112 (s, $\text{O}-\text{CH}_2$) cm^{-1} . Since the content of MDR-1 is very low with respect to the polymer matrix, it is very difficult to visualize the bands corresponding to the amino (R_2N), nitro (NO_2), and azo ($\text{N}=\text{N}$) groups. However, the presence of the band at 1652 cm^{-1} , due to the phenyl rings of the azobenzene moieties, which is not present in the FTIR spectrum of the polymer matrix, confirms that the azobenzene chromophore has been incorporated in this copolymer.

The optical properties of the polymers were studied by UV-Vis spectroscopy and the absorption spectra of the copolymers bearing different MDR-1 contents are shown in Figure 5. As it could be expected, all polymers exhibited a maximum absorption band around 450–470 nm, whose intensity increases with the azobenzene content. To get a deeper insight in the optical properties of the polymers, we compared the absorption spectrum of the PEGDA/MDR-1 (0.75

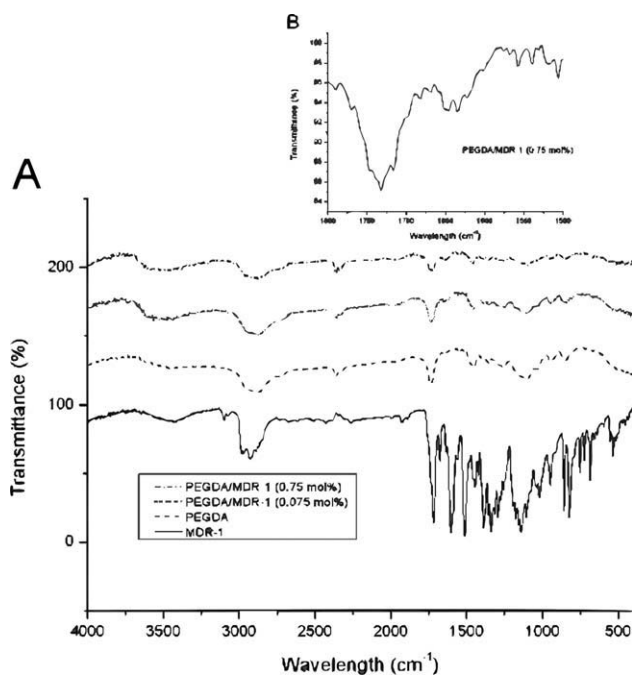


FIGURE 4 (a) FTIR analysis of PEGDA polymer matrix and the copolymers with different MDR-1 concentrations [0.075 and 0.75 mol %] [BPO: 2.4 mol %]. (b) For better analysis, an amplification of the FTIR spectrum of PEGDA/MDR1 0.75% is also included.

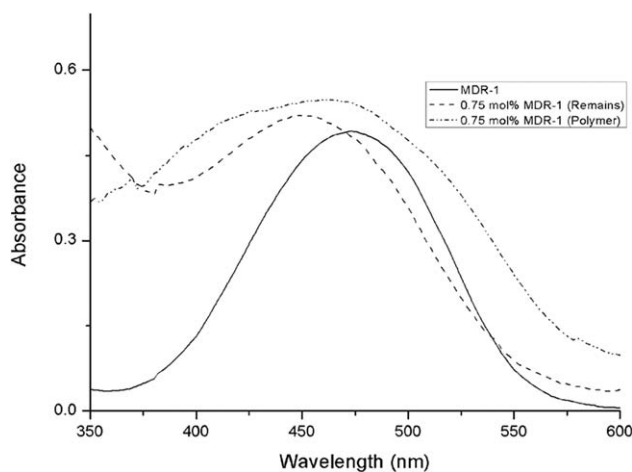


FIGURE 5 UV spectra of the azo-monomer (MDR-1) and of copolymer PEGDA/MDR-1 with the highest azo-monomer concentration [0.75 mol %] [BPO: 2.4 mol %].

mol %) with those of the MDR-1 monomer and the oligomer isolated during the soxhlet extraction. As we can see, the absorption spectrum of the MDR-1 monomer in CHCl_3 solution shows a well defined maximum absorption band at $\lambda_{\text{max}} = 473$ nm as other amino-nitro substituted azobenzenes, belonging to the pseudostilbenes category according to Rau's classification.⁶⁰ This kind of azobenzenes exhibits a total overlap of the $\pi-\pi^*$ and $n-\pi^*$ bands, which are inverted in the energy scale.⁵⁶ Similarly, the oligomer exhibited a well defined band at $\lambda_{\text{max}} = 452$ nm, which is 21 nm blue shifted with respect to the corresponding monomer. This hypsochromic effect reveals the presence of H-aggregates (parallel interactions) between the azobenzene groups in the oligomer. Further, ^1H NMR experiments (not shown) confirmed that such oligomers possess relatively high azobenzene content.

On the other hand, the PEGDA/MDR-1 (0.75 mol %) copolymer exhibited a broad absorption band centered at $\lambda_{\text{max}} = 460$ nm, which is 13 nm blue shifted when compared with that of the monomer. However, the presence of an additional blue shifted band at 415 nm as well as the presence of a discrete shoulder at 510 nm, reveals the presence of H-aggregates and traces of J-aggregates, respectively. It is very well known that polymers bearing donor-acceptor substituted azobenzenes tend to form antiparallel pairs to reach certain neutrality and stability. This behavior was previously reported in the literature for other azo-polymers.⁶³ According to the UV-Vis spectra shown in Figure 5, the PEGDA/MDR-1 (0.75 mol %) copolymer shows the presence of H-aggregation, which was not observed for the MDR-1 monomer.

Regarding the NLO properties and given the amorphous nature of the obtained materials, the PEGDA/MDR-1 copolymer sample with highest MDR-1 content (0.75 mol %) was selected for cubic NLO-characterization. The thickness of the studied sample (sandwiched PEGDA/MDR-1 film prepared within two glass slices) was ~ 27 μm . Figure 6(a) shows the

linear absorption coefficients evaluated within the visible range for this sample. Indeed, the Lambert-Beer law applies for such semitransparent film allowing an adequate data analysis and making this copolymer a potential candidate for some optical applications due to its appropriate transparency. It is evident from Figure 6(a) that the highest absorptive properties occur within the 400–580 nm spectral range, which may indicate additional conjugation of delocalized π -electrons provided by the higher content of MDR-1

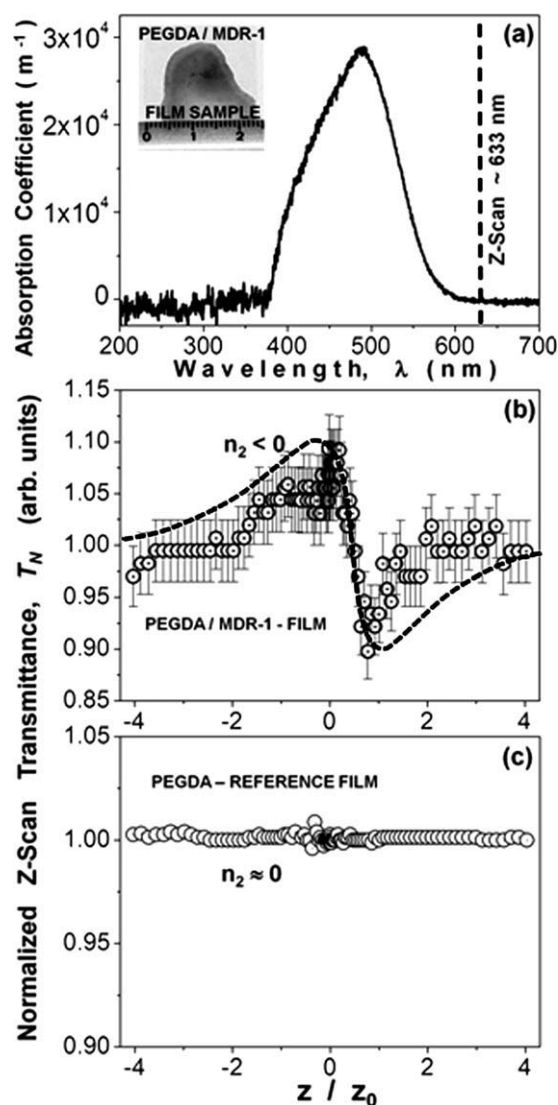


FIGURE 6 Linear and NLO measurements obtained for the pristine PEGDA hosting matrix and the PEGDA/MDR-1 copolymer sample with higher MDR-1 content (0.75 mol %; prepared film samples): (a) Absorption coefficients of the PEGDA/MDR-1 copolymer film evaluated within the visible range, (b) closed aperture Z-Scan data and theoretical fitting (dashed line) obtained at $\lambda_{\text{Z-Scan}} = 632.8$ nm for the PEGDA/MDR-1 film sample (an estimated experimental error below 5% is also considered for the Z-Scan data: error bars), and (c) closed aperture Z-Scan data obtained for a pristine PEGDA reference sample under similar experimental conditions.

chromophores within this sample. This suggestion was explored by means of NLO Z-Scan experiments as explained below. Under this framework, the available laser excitation line for Z-Scan experiments ($\lambda_{\text{Z-Scan}} = 632.8 \text{ nm}$) is also depicted in this figure (vertical dashed line). At this wavelength, lowest absorption conditions occur, allowing nonresonant NLO-characterizations of the sample which is a critical point when working with low T_g -based organic materials. In fact, a small linear absorption coefficient in the order of $\alpha_0 \approx 59.13 \text{ m}^{-1}$ was evaluated for the studied copolymer at $\lambda_{\text{Z-Scan}}$. This value is very useful for the determination of the nonlinear refraction and absorption coefficients according to the Z-Scan technique. Additionally, the linear refractive index of this material was estimated to be $n_0 \approx 1.5738$.

Z-Scan measurements were performed at room conditions on the PEGDA/MDR-1 prepared film. The observed nonlocal effect of this sample is shown in Figure 6(b). A rigorous theoretical fitting was performed to evaluate both the nonlinear absorptive and refractive properties of this sample. The NLO-response of the developed copolymer was characterized by varying the polarization input planes of the He-Ne laser system to explore microscopic material asymmetries or anisotropies throughout the sample structure. In general, since all NLO-measurements were systematically performed with different laser input polarization states (from 0 to 90°: *s*-polarization to *p*-polarization, respectively) and the obtained curves are quite similar in each sample, the film structures do not seem to show any significant anisotropic behavior, thus confirming their amorphous nature. On the other hand, the Z-Scan curve for a pristine, highly transparent, PEGDA reference sample [Fig. 6(c)] exhibits negligible nonlinear refraction and absorption when compared with the curves obtained for the PEGDA/MDR-1 system at the same laser power regime. Taking into account the theory developed by Sheik-Bahae and coworkers and Liu et al.,^{64–69} it is observed from our measurements that the nonlinear refractive response of the studied sample can be unambiguously determined by a typical peak-to-valley transmittance curve. Hence, one can immediately observe that the PEGDA/MDR-1 copolymer sample (0.75 mol % MDR-1) exhibits a negative NLO-refraction coefficient ($\gamma < 0$).

The respective theoretical fit (TF) to the obtained Z-Scan transmission data (solid lines) are also shown in Figure 6(b). To perform the TF according to previous theoretical studies, the normalized Z-Scan transmittance T_N can be determined as a function of the dimensionless sample position ($x = z/z_0$), where z_0 is the Rayleigh range and z is the Z-Scan sample position. Hence, the TF was obtained according to the following equation, considering both nonlinear refraction and absorption effects.⁶⁹

$$T_N \approx 1 + [4x/(1+x^2)(9+x^2)]\Delta\Phi - [2(x^2+3)/(1+x^2)(9+x^2)]\Delta\Psi. \quad (1)$$

Here, the first term is related to NLO-refractive effects, whereas the second one is associated to NLO-absorptive phenomena. Indeed, as the obtained Z-Scan data [Fig. 6(b)]

clearly exhibit a peak-to-valley transmittance asymmetry, NLO absorption effects are expected.⁶⁹ The fitting parameters are in this case the induced phase shifts $\Delta\Phi$ or $\Delta\Psi$, respectively. In the former case, the phase shift is given by $\Delta\Phi = 2\pi\gamma I_0 L_{\text{eff}}/\lambda$,⁶⁷ from which the NLO refractive index (γ -coefficient) can be obtained. In the latter case, the phase shift is provoked by the NLO-absorption and is given by $\Delta\Psi = \beta I_0 L_{\text{eff}}/2$,⁶⁵ allowing the evaluation of the NLO absorption (β -coefficient), either due to two photon (or multiphoton) absorption and/or saturable absorption. In these equations, λ is the laser wavelength, I_0 is the input beam intensity (at focal spot: $z = 0$), and L_{eff} is the effective thickness of the film sample, defined as $L_{\text{eff}} = [1 - (e^{-\alpha_0 L_s})](\alpha_0)^{-1}$, where α_0 represents the linear absorption coefficient. All these equations are well established and have been proven in early Z-Scan works.^{64–69} The theoretical restrictions imposed by these formulas to apply such expressions at optimal conditions ($|\Delta\Phi_0| < \pi$, $S \approx 20\%$, etc.) are not always fully satisfied in our experimental result due to the large phase shifts and huge nonlinearities. Nevertheless, in most cases (mainly in the case of well defined $\gamma > 0$ or $\gamma < 0$ curves); our results nearly satisfy these conditions and can be conveniently fitted according to these theoretical formulas. Thus, for comparison purposes and to be consistent with the estimation of the γ -values and β -values, we assumed their applicability and used them in our experimental results. The TF allowed us to evaluate a positive NLO-refractive coefficient of $\gamma = -2.14 \times 10^{-10} \text{ m}^2 \text{ W}^{-1}$ (or $n_2 = -8.057 \times 10^{-4} \text{ esu}$) and a NLO absorption coefficient of $\beta = +8.69 \times 10^{-5} \text{ m W}^{-1}$. The obtained γ/n_2 -values are very large, many orders of magnitude larger than those observed for typical glass substrates or for the classical CS₂ standard reference material: $+1.2 \times 10^{-11} \text{ esu}$ (Z-Scan at $\lambda = 10.6 \text{ }\mu\text{m}$) or $6.8 \times 10^{-13} \text{ esu}$ (degenerate four wave mixing at $\lambda = 532 \text{ nm}$).^{64–68} On the other hand, the positive sign obtained for the β -coefficient reveals the nature of the NLO absorptive phenomena of our sample, indicating strong multiphoton absorption effects.^{64–69} This fact indicates the onset of thermal effects during Z-Scan experiments due to long cw-laser irradiation and low T_g -values of the samples. Indeed, Z-Scan experiments were performed at extremely low laser energy conditions ($\sim 3 \text{ mW}$) to avoid photodegradation effects on the sample, which started at power regimens in the order of $\sim 5 \text{ mW}$.

EXPERIMENTAL

Materials

PEGDA ($M_n \cong 575$, $d = 1.12 \text{ g mL}^{-1}$), triethylamine (TEA, formula weight (FW) = 101.19, bp = 88.8 °C, $d = 0.726 \text{ g mL}^{-1}$), and Disperse Red-1 dye (DR-1, FW = 314.34, mp = 160–162 °C) were purchased from Sigma-Aldrich. BPO (FW = 242.23, mp = 102–105 °C) and methacryloyl chloride (MAcC, FW = 104.53, bp = 95–96 °C, $d = 1.07 \text{ g mL}^{-1}$) were purchased from Fluka. All reagents were used as received, without further purification.

Synthesis of MDR-1

DR-1 (0.72 g, 2.28 mmol) was dissolved in freshly distilled THF (12 mL) under argon atmosphere; then TEA (0.33 g,

3.32 mmol) was added to the solution with a syringe. The mixture was cooled in an ice bath and MAcC (0.29 g, 2.76 mmol), dissolved in THF, (4 mL) and was added drop wise by means of an addition funnel. The reaction mixture was stirred for 24 h at room temperature. The resulting product was extracted with chloroform, dried with anhydrous MgSO_4 , and concentrated at reduced pressure. Then, the crude product was purified by flash column chromatography on silica gel, using an appropriate mixture hexane–chloroform as eluent. Pure MDR-1 monomer (Fig. 1) was obtained as a dark red solid with good yield (75%). The structure of MDR-1 was confirmed by FTIR and ^1H NMR spectroscopies and the observed signals correspond to those previously reported in the literature.^{70,71}

IR (KBr): $\nu = 3090$ (s, C–H aromatic and vinylic), 2961 (s, CH_2), 2924 (s, CH_2 and CH_3), 1727 (s, C=O), 1603 (s, C=C aromatic), 1516 (s, NO_2), 1447 (s, N=N), 1378, 1337 (s, C–O of the ester), 1261 (s, C–N), 1099 (s, O– CH_2), 856 (out of plane, = CH_2 vinylic), 802 (out of plane, =C–H aromatic) cm^{-1} .

^1H -NMR (CDCl_3 , 400 MHz): $\delta = 8.33$ (d, 2H, $J = 9.06$ Hz, H^4); 7.93 (d, 2H, $J = 9.06$ Hz, H^3); 7.91 (d, 2H, $J = 8.81$ Hz, H^2); 6.83 (d, 2H, $J = 9.32$ Hz, H^1); 6.12 (s, 2H, H^5 , $J_1 = 1.76$); 5.60 (s, 1H, H^6 , $J_1 = 1.51$); 4.38 (t, 2H, $J_1 = 6.29$ Hz, $J_2 = 6.29$ Hz, COO– CH_2); 3.74 (t, 2H, $J_1 = 6.29$ Hz, $J_2 = 6.29$, NCH_2), 3.56 (t, 2H, $J_1 = 7.05$ Hz, $J_2 = 7.05$ NCH_2CH_3); 1.95 (s, 3H, CH_3 of methacrylate); 1.27 (t, 3H, $J_1 = 7.05$ Hz, $J_2 = 7.05$, $\text{NCH}_2\text{—CH}_3$) ppm.

FP Experiments

In a glass test tube (16 cm length, 16 mm inner diameter), suitable amounts of PEGDA, MDR-1, and BPO were mixed until all BPO was completely dissolved (Table 1). Caution: FP experiments carried out with more than 7.1 mol % BPO resulted in test tube explosion!

The test tubes containing the mixture were locally heated at the top level of the solution, using a soldering iron as heating source, until the formation of a propagating front was observed. The heat released during the conversion of the monomer into polymer was responsible for the formation of a hot polymerization front, able to self-sustain, and propagate throughout the whole tube. Front velocity (± 0.05 cm min^{-1}) and front maximum temperature (± 15 $^\circ\text{C}$) were recorded.

Characterization

Temperature profiles were measured using a K-type thermocouple placed into the monomer mixture at 2 cm (± 0.5 cm) from the bottom of the tube. It was connected to a digital thermometer (Delta Ohm 9416) for temperature reading and recording. The position of the front, easily visible through the glass walls of the tube, was measured as a function of the time.

DSC measurements were conducted in a DSC Q100 Waters TA Instrument. For each sample, two consecutive scans were carried out from -80 to $+300$ $^\circ\text{C}$ with a heating rate of 10 $^\circ\text{C min}^{-1}$, under argon atmosphere. Monomer conversion

was determined from the first thermal scan, whereas T_g values were determined from the second scan (Table 1). TGA measurements were performed using a TA Instrument thermobalance TGA 2050, under air flow, from 25 to 500 $^\circ\text{C}$ at a heating rate of 10 $^\circ\text{C min}^{-1}$.

FTIR spectra of the samples in KBr pressed pellets were recorded in a Fourier transform infrared spectroscope (JASCOFT 480 spectrometer), carrying out 16 scans at a resolution of 4 cm^{-1} . UV-Vis spectra of the polymers were carried out in a Hitachi U-2010 spectrometer (1 cm quartz cell). The MDR-1 concentration of all samples was calculated by absorption spectroscopy and the extinction coefficient for this monomer was estimated to be $46,700$ M cm^{-1} in CHCl_3 .

Finally, due to the amorphous structure of the resulting PEGDA/MDR-1 copolymers, these systems were also studied as active media for cubic $\chi^{(3)}$ -NLO effects such as nonlinear refraction and absorption via Z-Scan measurements.⁷² The experimental Z-Scan set-up was implemented using an unpolarized laser beam from a 35-mW He-Ne laser system working at 632.8 nm (THORLABS, HRR170-1). Its energy was carefully monitored and kept constant during long Z-Scan measurements. The spatial mode of the laser beam was close to Gaussian TEM_{00} . The polarization plane of the He-Ne laser beam was adjusted and controlled by means of a linear polarizer mounted on a rotation stage. The polarized laser beam was focused on the sample by means of a positive lens ($f = 5$ cm), so that a light power density of approximately 8.53×10^6 W m^{-2} reached the studied sample at the focal spot. At last, the samples were mounted on a motorized translation stage (25 mm length travel in steps of 2 μm) to perform Z-Scan experiments within the optical focal range. A large area Si-photodetector (EOT ET-2040) was located at ~ 0.96 m from the focusing lens, after a 2.5-mm diameter (20% transmittance) diaphragm-aperture. All NLO-signals captured from photodetectors were measured with a digital oscilloscope (Tektronix TDS, 744A), and all motion systems and set-up management were automated via a LabView control program.

CONCLUSIONS

For the first time, the frontal copolymerization of an azo-monomer was carried out. MDR-1 was copolymerized with PEGDA. The influence of the amounts of MDR-1 and initiator was studied to determine the optimum concentration range in which FP can occur. Azo-polymers containing up to 0.75 mol % of MDR-1 were successfully obtained. Such concentration is good enough to confer their interesting NLO properties. The UV-Vis spectra of the polymers exhibit a significant blue shift of the absorption bands with respect to MDR-1 monomer, due to the formation of H-aggregates. Outstanding cubic NLO effects were measured in the PEGDA/MDR-1 copolymer sample with higher MDR-1 content (0.75 mol %) via the Z-Scan technique, where high NLO-refractive coefficients in the order of 10^{-4} esu were found. This remarkable NLO activity was mainly due to the MDR-1 azo-compound as the reference PEGDA sample did not exhibit any NLO-response at same experimental conditions, acting only as an

adequate mechanical hosting matrix. In addition, the NLO-absorptive response of the studied material was established as a multiphoton process. However, more NLO investigations should be performed in these materials to further understand the electronic and thermal contributions to the cubic nonlinearities. Additionally, complementary studies on the MDR-1 chromophore loading in these kinds of PEGDA-based copolymers and other systems should also be performed order to improve both the NLO-response and thermal properties for stable NLO-applications (including quadratic NLO-effects for eclectically poled film samples). Some of these experiments are currently underway and will be presented in a future work.

We thank Miguel Angel Canseco and Gerardo Cedillo for their assistance with absorption and NMR spectroscopies, respectively. Javier Illescas and Yessica S. Ramirez-Fuentes are grateful to CONACyT for scholarship. We also thank Henkel Co., the Instituto de Ciencia y Tecnología del Distrito Federal (ICyTDF), and the Italian Ministry of University and Scientific Research for financial support.

REFERENCES AND NOTES

- Chechilo, N. M.; Khvilivitskii, R. J.; Enikolopyan, N. S. *Dokl Akad Nauk SSSR* 1972, 204, 1180–1181.
- Davtyan, S. P.; Zhirkov, P. V.; Vol'fson, S. A. *Russ Chem Rev* 1984, 53, 150–163.
- Davtyan, S. P.; Surkov, N. F.; Rozenberg, B. A.; Enikolopyan, N. S. *Dokl Phys Chem* 1977, 32, 64–67.
- Pojman, J. A.; Ilyashenko, V. M.; Khan, A. M. *J Chem Soc Faraday Trans* 1996, 92, 2825–2837.
- Pojman, J. A.; Elclan, W.; Khan, A. M.; Mathias, L. *J Polym Sci Part A: Polym Chem* 1997, 35, 227–230.
- Pojman, J. A.; Masere, J.; Pettre, E.; Rustici, M.; Volpert, V. *Chaos* 2002, 12, 56–65.
- McFarland, B.; Popwell, S.; Pojman, J. A. *Macromolecules* 2006, 39, 53–63.
- McFarland, B.; Popwell, S.; Pojman, J. A. *Macromolecules* 2004, 37, 6670–6672.
- Nason, C.; Roper, T.; Hoyle, C.; Pojman, J. A. *Macromolecules* 2005, 38, 5506–5512.
- Pojman, J. A. *J Am Chem Soc* 1991, 113, 6284–6286.
- Khan, A. M.; Pojman, J. A. *Trends Polym Sci* 1996, 4, 253–257.
- Fortenberry, D. I.; Pojman, J. A. *J Polym Sci Part A: Polym Chem* 2000, 38, 1129–1135.
- Nason, C.; Pojman, J. A.; Hoyle, C. *J Polym Sci Part A: Polym Chem* 2008, 46, 8091–8096.
- Pojman, J. A.; Chen, L. *J Polym Sci Part A: Polym Chem* 2006, 44, 3018–3024.
- Mariani, A.; Fiori, S.; Chekanov, Y.; Pojman, J. A. *Macromolecules* 2001, 34, 6539–6541.
- Chekanov, Y.; Arrington, D.; Brust, G.; Pojman, J. A. *J App Polym Sci* 1997, 66, 1209–1216.
- Scognamillo, S.; Bounds, C.; Luger, M.; Mariani, A.; Pojman, J. A. *J Polym Sci Part A: Polym Chem* 2010, 48, 2000–2005.
- Jimenez, Z.; Pojman, J. A. *J Polym Sci Part A: Polym Chem* 2007, 45, 2745–2754.
- Fiori, S.; Malucelli, G.; Mariani, A.; Ricco, L.; Casazza, E. *e-Polymers* 2002, 057, 1–10.
- Mariani, A.; Fiori, S.; Bidali, S.; Alzari, V.; Malucelli, G. *J Polym Sci Part A: Polym Chem* 2008, 46, 3344–3351.
- Fiori, S.; Mariani, A.; Ricco, L.; Russo, S. *Macromolecules* 2003, 36, 2674–2679.
- Mariani, A.; Bidali, S.; Fiori, S.; Malucelli, G.; Sanna, E. *e-Polymers* 2003, 044, 1–9.
- Mariani, A.; Bidali, S.; Caria, G.; Monticelli, O.; Russo, S.; Kenny, J. M. *J Polym Sci Part A: Polym Chem* 2007, 45, 2204–2212.
- Mariani, A.; Alzari, V.; Monticelli, O.; Pojman, J. A.; Caria, G. *J Polym Sci Part A: Polym Chem* 2007, 45, 4514–4521.
- Fiori, S.; Mariani, A.; Ricco, L.; Russo, S. *e-Polymers* 2002, 029, 1–10.
- Mariani, A.; Fiori, S.; Pedemonte, E.; Pincin, S.; Princi, E.; Vicini, S. *ACS Polym Prepr* 2002, 43, 869–870.
- Mariani, A.; Bidali, S.; Cappelletti, P.; Caria, G.; Colella, A.; Brunetti, A.; Alzari, V. *e-Polymers* 2009, 064, 1–12.
- Brunetti, A.; Princi, E.; Vicini, S.; Pincin, S.; Bidali, S.; Mariani, A. *Nucl Instrum Meth B* 2004, 222, 235–241.
- Vicini, S.; Mariani, A.; Princi, E.; Bidali, S.; Pincin, S.; Fiori, S.; Pedemonte, E.; Brunetti, A. *Polym Adv Technol* 2005, 16, 293–298.
- Caria, G.; Alzari, V.; Monticelli, O.; Nuvoli, D.; Kenny, J. M.; Mariani, A. *J Polym Sci Part A: Polym Chem* 2009, 47, 1422–1428.
- Gavini, E.; Mariani, A.; Rassa, G.; Bidali, S.; Spada, G.; Bonferoni, M. C.; Giunchedi, P. *Eur Polym J* 2009, 45, 690–699.
- Alzari, V.; Monticelli, O.; Nuvoli, D.; Kenny, J. M.; Mariani, A. *Biomacromolecules* 2009, 10, 2672–2677.
- Scognamillo, S.; Alzari, V.; Nuvoli, D.; Mariani, A. *J Polym Sci Part A: Polym Chem* 2010, 48, 2486–2490.
- Alzari, V.; Mariani, A.; Monticelli, O.; Valentini, L.; Nuvoli, D.; Piccinini, M.; Scognamillo, S.; Bittolo Bon, S.; Illescas, J. *J Polym Sci Part A: Polym Chem* 2010, 48, 5375–5381.
- Scognamillo, S.; Alzari, V.; Nuvoli, D.; Mariani, A. *J Polym Sci Part A: Polym Chem* 2010, 48, 4721–4725.
- Cai, X.; Chen, S.; Chen, L. *J Polym Sci Part A: Polym Chem* 2008, 46, 2177–2185.
- Hu, T.; Chen, S.; Tian, Y.; Chen, L.; Pojman, J. A. *J Polym Sci Part A: Polym Chem* 2007, 45, 873–881.
- Chen, L.; Hu, T.; Yu, H.; Chen, S.; Pojman, J. A. *J Polym Sci Part A: Polym Chem* 2007, 45, 4322–4330.
- Chen, S.; Tian, Y.; Chen, L.; Hu, T. *Chem Mater* 2006, 18, 2159–2163.
- Chen, S.; Sui, J.; Chen, L.; Pojman, J. A. *J Polym Sci Part A: Polym Chem* 2005, 43, 1670–1680.
- Fang, Y.; Chen, L.; Wang, C. F.; Chen, S. *J Polym Sci Part A: Polym Chem* 2010, 48, 2170–2177.

- 42** Tu, J.; Zhou, J.; Wang, C.; Zhang, Q.; Chen, S. *J Polym Sci Part A: Polym Chem* 2010, 48, 4005–4012.
- 43** Tu, J.; Chen, L.; Fang, Y.; Wang, C.; Chen, S. *J Polym Sci Part A: Polym Chem* 2010, 48, 823–831.
- 44** Falk, B.; Vallinas, S. M.; Crivello, J. *J Polym Sci Part A: Polym Chem* 2003, 41, 579–596.
- 45** Bulut, U.; Crivello, J. *J Polym Sci Part A: Polym Chem* 2005, 43, 3205–3220.
- 46** Crivello, J.; Lee, J. L. *J Polym Sci Part A: Polym Chem* 1989, 27, 3951–3968.
- 47** Crivello, J.; Bulut, U. *Design Monom Polym* 2005, 8, 517–531.
- 48** Alzari, V.; Nuvoli, D.; Scognamillo, S.; Piccinini, M.; Gioffredi, E.; Malucelli, G.; Marceddu, S.; Sechi, M.; Sanna, V.; Mariani, A. *J Mater Chem*, in press (doi: 10.1039/c1jm11076d).
- 49** Cruise, G. M.; Scharp, D. S.; Hubbell, J. A. *Biomaterials* 1998, 19, 1287–1294.
- 50** Mellott, M. B.; Searcy, K.; Pishko, M. V. *Biomaterials* 2001, 22, 929–941.
- 51** Hu, X.; Zheng, P. J.; Zhao, X. Y.; Li, L.; Tam, K. C.; Gan, L. H. *Polymer* 2004, 45, 6219–6225.
- 52** Delaire, J. A.; Nakatani, K. *Chem Rev* 2000, 100, 1817–1846.
- 53** Takashima, Y.; Nakayama, T.; Miyauchi, M.; Kawaguchi, Y. *Chem Lett* 2004, 33, 890–891.
- 54** Ikeda, T.; Ooya, T.; Yui, N. *Polym J.* 1999, 31, 658–663.
- 55** Tung, C. H.; Wu, L. Z.; Zhang, L. P.; Chen, B. *Acc Chem Res* 2003, 36, 39–47.
- 56** Natansohn, A.; Rochon, P. *Chem Rev* 2002, 102, 4139–4175.
- 57** Freiberg, S.; Lagugné-Labarthe, F.; Rochon, P.; Natansohn, A. *Macromolecules* 2003, 36, 2680–2688.
- 58** Rivera, E.; Carreón-Castro, M. P.; Salazar, R.; Huerta, G.; Becerril, C.; Rivera, L. *Polymer* 2007, 48, 3420–3428.
- 59** Meng, X.; Natansohn, A.; Rochon, P.; Barrett, C. *Macromolecules* 1996, 26, 946–952.
- 60** Shin, D. M.; Schanze, K. S.; Whitten, D. G. *J Am Chem Soc* 1989, 111, 8494–8501.
- 61** Kasha, M. *Radiat Res* 1963, 20, 55–71.
- 62** Tochina, E. M.; Postinkov, L. M.; Shylapintokh, V. Ya.; Gritskov, A. M.; Belousova, G. A.; Bryuske, Ya. E. *Inst Chem Phys Acad Sci USSR* 1969, 4, 818.
- 63** Iftime, G.; Lagugné-Labarthe, F.; Natansohn, A.; Rochon, P. *J Am Chem Soc* 2000, 122, 12646–12650.
- 64** Sheik-Bahae, M.; Said, A. A.; Van Stryland, E. W. *Opt Lett* 1989, 14, 955–957.
- 65** Sheik-Bahae, M.; Said, A. A.; Hagan, D. J.; Soileau, M. J.; Van Stryland, E. W. *Opt Eng* 1991, 30, 1228–1235.
- 66** Sheik-Bahae, M.; Said, A. A.; Wei, T. H.; Hagan, D. J.; Van Stryland, E. W. *IEEE J Quant Electron* 1990, 26, 760–769.
- 67** Xia, T.; Hagan, D. J.; Sheik-Bahae, M.; Van Stryland, E. W. *Opt Lett* 1994, 19, 317–319.
- 68** *Nonlinear Optics of Organic Molecules and Polymers*; Nalwa, H. S.; Miyata, S., Eds.; CRS Press: Boca Raton, FL, 1997.
- 69** Liu, X.; Guo, S.; Wang, H.; Hou, L. *Opt Comm* 2001, 197, 431–437.
- 70** Rochon, P.; Gosselin, J.; Natansohn, A.; Xie, S. *Appl Phys Lett* 1992, 60, 4–5.
- 71** Natansohn, A.; Rochon, P.; Gosselin, J.; Xie, S. *Macromolecules* 1992, 25, 2268–2273.
- 72** Rodríguez-Rosales, A. A.; Morales-Saavedra, O. G.; Román, C. J.; Ortega-Martínez, R. *Opt Mat* 2008, 31, 350–360.